

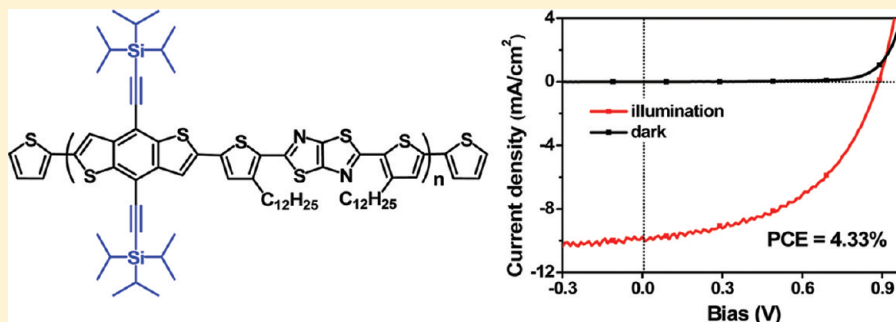
## A Copolymer of Benzodithiophene with TIPS Side Chains for Enhanced Photovoltaic Performance

Qinqin Shi,<sup>†</sup> Haijun Fan,<sup>†</sup> Yao Liu,<sup>†</sup> Wenping Hu, Yongfang Li, and Xiaowei Zhan\*

Beijing National Laboratory for Molecular Sciences and Key Laboratory of Organic Solids, Institute of Chemistry, Chinese Academy of Sciences, Beijing 100190, China

Supporting Information

## ABSTRACT:



A new conjugated copolymer PBDTTT-TIPS containing thiazolothiazole acceptor unit and triisopropylsilylethynyl (TIPS)-functionalized benzodithiophene donor unit was synthesized by Pd-catalyzed Stille coupling and compared with its alkoxy-substituted analogue PBDTTT-C12. PBDTTT-TIPS exhibits decomposition temperature of 377 °C, absorption maximum of 598 nm, HOMO level of  $-5.3$  eV, and hole mobility as high as  $1.2 \times 10^{-3} \text{ cm}^2 \text{ V}^{-1} \text{ s}^{-1}$ . Without any post-treatments, polymer solar cells based on the blend of PBDTTT-TIPS and PC<sub>71</sub>BM exhibited power conversion efficiency as high as 4.33%, which is 2 times that for device based on the PBDTTT-C12:PC<sub>71</sub>BM blend. TIPS and C12 side chains exhibit a little impact on absorption, HOMO level, and hole mobility of the polymers, but they significantly influence blend film morphology and photovoltaic performance. TIPS side chains induces excellent compatibility between PBDTTT-TIPS and PC<sub>71</sub>BM, and the PBDTTT-TIPS:PC<sub>71</sub>BM blend exhibits perfect phase separation scales around 10–20 nm, which is beneficial to charge separation and enhanced efficiency of the device, while C12 side chains leads to large phase separation, which is responsible for the lower efficiency.

## INTRODUCTION

Polymer solar cells (PSCs) have attracted increasing attention because they have shown promising potential as a result of their unique advantages such as low cost, light weight, and large-area fabrication on flexible substrates.<sup>1</sup> Recently, great advances have achieved in development of novel photovoltaic polymers and device structures.<sup>2–12</sup> The power conversion efficiencies (PCEs) can now reach 7–8%.<sup>13–18</sup> It is worthy of mentioning that the large planar benzo[1,2-*b*:4,5-*b'*]dithiophene (BDT) unit has emerged as an attractive building block for high-efficiency photovoltaic polymers.<sup>13,15–18</sup> For solution processing, the use of long alkyl or alkoxy side chains has been a common approach to modify the BDT unit.<sup>15–17,19–22</sup> However, the side-chain nature not only affects the molecular weight and solubility of the polymers but also affects the absorption, energy levels, and charge transport properties.<sup>23–29</sup> In particular, the side chain affects morphology of blends of polymer donors and fullerene acceptors and finally affects the photovoltaic performance of devices.<sup>23–29</sup> In order to further improve solar cell efficiency, it is necessary to explore other type side chains to modify the BDT unit, for example, thiophene side chains.<sup>18,30,31</sup>

Bulky triisopropylsilylethynyl (TIPS) groups on acene derivatives not only improve the solubility and oxidative stability of the semiconductors but also promote the  $\pi$ -orbital overlap. As a result, TIPS-functionalized acenes gained importance as a class of highly soluble, air-stable, high-performance p-type organic semiconductors.<sup>32,33</sup> The small molecules and polymers based on TIPS-substituted acenes were also used in organic photovoltaic cells as electron donors or acceptors with PCEs as high as 2.25%.<sup>34–37</sup> Stefan and co-workers reported synthesis of polymers based on phenylethynyl-substituted BDT and their application in PSCs with PCEs up to 1.05%.<sup>28</sup> Watson and co-workers reported synthesis of a small molecule based on TIPS-substituted BDT unit but not any device applications.<sup>38</sup> There have been no reports on small molecules or polymers based on TIPS-functionalized BDT unit for organic solar cells.

Thiazolothiazole (TT) has a rigid and coplanar fused ring and thereby could facilitate highly extended  $\pi$ -electron system and

Received: August 27, 2011

Revised: October 20, 2011

Published: November 10, 2011

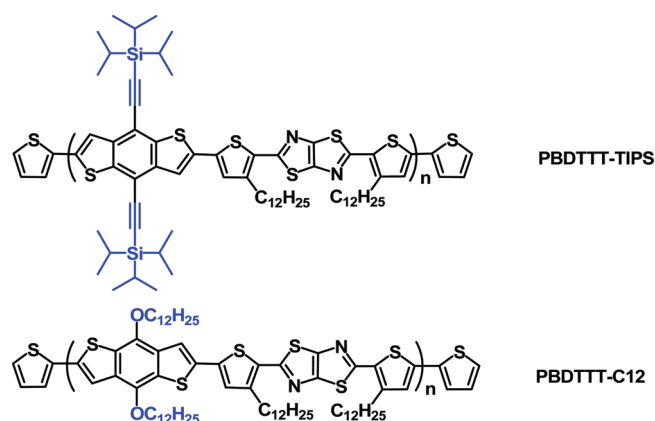


Figure 1. Chemical structures of BDT-TT copolymers.

strong  $\pi$ -stacking. As a result, conjugated small molecules and polymers based on thiazolothiazole exhibited high charge carrier mobilities up to  $0.3 \text{ cm}^2 \text{ V}^{-1} \text{ s}^{-1}$ .<sup>39–41</sup> Recently, several copolymers of thiazolothiazole with fused-ring donor building blocks such as benzodithiophene, cyclopentadithiophene, carbazole, or dithienosilole were synthesized for PSC applications, and PCEs up to 5.88% were reported.<sup>42–49</sup>

In this paper, we designed and synthesized a copolymer of TIPS-functionalized BDT and TT (PBDTTT-TIPS, Figure 1) and compared with its alkoxy-substituted analogue PBDTTT-C12. Slight difference between these two polymers lies only on the side chains on BDT unit, while big difference in phase separation scale of the polymer donor/PC<sub>71</sub>BM blend films was observed. PSC devices based on PBDTTT-TIPS exhibit PCEs as high as 4.33% without post-treatments, which is double that for PBDTTT-C12-based solar cells.

## EXPERIMENTAL SECTION

**Measurements and Characterization.** The <sup>1</sup>H NMR spectra were measured on a Bruker AVANCE 400 MHz spectrometer using tetramethylsilane (TMS;  $\delta = 0$  ppm) as an internal standard. Elemental analyses were carried out using a FLASH EA1112 elemental analyzer. Thermogravimetric analysis (TGA) measurements were performed using a DTG-60 thermal analysis system under N<sub>2</sub> at a heating rate of  $20^\circ \text{C min}^{-1}$ . Solution (chloroform,  $10^{-6}$  M) and thin-film (on quartz substrate, spin-coated from chloroform solution) UV–vis spectra were recorded on a JASCO V-570 spectrophotometer. The electrochemical measurements were carried out under nitrogen on a deoxygenated solution of tetra-*n*-butylammonium hexafluorophosphate (0.1 M) in acetonitrile with a computer-controlled CHI660C electrochemical workstation, a glassy-carbon working electrode, a platinum-wire auxiliary electrode, and an Ag-wire anodized with AgCl as a pseudoreference electrode. Potentials were referenced to the ferrocenium/ferrocene ( $\text{FeCp}_2^{+/0}$ ) couple by using ferrocene as a standard. The gel permeation chromatography (GPC) measurements were performed on a Waters 515 chromatograph connected to a Waters 2414 refractive index detector, using THF as eluent and polystyrene standards as calibrants; three Waters Styragel columns (HT2, 3, 4) connected in series were used.

**OFET Device Fabrication and Characterization.** Field-effect transistors based on PBDTTT-TIPS polymer films were fabricated in a bottom gate, top contact configuration at ambient atmosphere. Highly *n*-doped silicon and thermally grown silicon dioxide (500 nm) were used as back gate and gate dielectric, respectively. The substrates were cleaned with pure water, hot concentrated sulfuric acid–hydrogen peroxide

solution (concentrated sulfuric acid/hydrogen peroxide water = 2:1), pure water, and pure isopropanol. Then vaporized octadecyltrichlorosilane (OTS) was used for surface modification of the gate dielectric layer.

Solution of PBDTTT-TIPS in *o*-dichlorobenzene (about  $10 \text{ mg mL}^{-1}$ ) was spin-coated onto OTS-treated substrates to form thin films. Prior to thermal evaporation of top contacts, the films were baked at  $120^\circ \text{C}$  in a vacuum chamber for 30 min to remove the residual solvent. Gold contacts (25 nm) for source and drain electrodes were vacuum-deposited at a rate of  $0.1 \text{ \AA s}^{-1}$  through a metal shadow mask that defined a series of transistor devices with a channel length ( $L$ ) of  $50 \mu\text{m}$  and a channel width ( $W$ ) of 1 mm. The characterization was accomplished by a Keithley 4200 SCS with a micromanipulator 6150 probe station in a clean shielded box at ambient atmosphere. Then field-effect mobility was calculated from the standard equation for saturation region in metal–dioxide semiconductor field-effect transistors:  $I_{\text{DS}} = (W/2L)\mu C_i(V_{\text{G}} - V_{\text{T}})^2$ , where  $I_{\text{DS}}$  is drain-source current,  $\mu$  is field-effect mobility,  $W$  and  $L$  are the channel width and length,  $C_i$  is the capacitance per unit area of the dielectric layer ( $C_i = 7.5 \text{ nF cm}^{-2}$ ),  $V_{\text{G}}$  is the gate voltage, and  $V_{\text{T}}$  is the threshold voltage.

**PSC Device Fabrication and Characterization.** The PSC devices were fabricated with a structure of ITO/PEDOT:PSS/PBDTTT-TIPS (or PBDTTT-C12):PC<sub>71</sub>BM/Ca/Al. The patterned ITO glass (sheet resistance =  $30 \Omega \square^{-1}$ ) was precleaned in an ultrasonic bath of acetone and isopropanol and treated in ultraviolet-ozone chamber (Jelight Co.) for 0.5 h. A thin layer (30 nm) of poly(3,4-ethylenedioxythiophene):poly(styrenesulfonate) (PEDOT:PSS, Baytron P VP AI 4083, Germany) was spin-coated onto the ITO glass and baked at  $150^\circ \text{C}$  for 0.5 h. A solution of PBDTTT-C12/PC<sub>71</sub>BM (1:2, w/w) or a solution of PBDTTT-TIPS/PC<sub>71</sub>BM (1:1 or 1:2, w/w) in chloroform or chlorobenzene was subsequently spin-coated on the surface of PEDOT:PSS layer to form a photosensitive layer. Calcium (ca. 15 nm) and aluminum (ca. 50 nm) layers were subsequently evaporated onto the surface of the photosensitive layer under vacuum (ca.  $10^{-5}$  Pa) to form the cathode. The active area of the device was  $4 \text{ mm}^2$ . Current–voltage curve was measured with a computer-controlled Keithley 236 source measure unit. A xenon lamp coupled with AM 1.5 solar spectrum filters was used as the light source, and the optical power at the sample was  $100 \text{ mW cm}^{-2}$ . The incident photon-to-current conversion efficiency (IPCE) spectrum was measured by Stanford Research Systems model SR830 DSP lock-in amplifier coupled with WDG3 monochromator and 500 W xenon lamp.

**Materials.** 2,5-Bis(3-dodecyl-5-(trimethylstannyl)thiophen-2-yl)-thiazolo[5,4-*d*]thiazole,<sup>41</sup> 2,6-dibromo-4,8-bis(triisopropylsilyl)ethynylbenzo[1,2-*b*:4,5-*b'*]dithiophene,<sup>50</sup> and PBDTTT-C12<sup>42</sup> were synthesized according to the literature methods. Toluene was distilled from sodium benzophenone under nitrogen before use. Unless stated otherwise, the other reagents were purchased from commercial sources, and used without further purification.

**Poly{(4,8-bis(triisopropylsilyl)ethynyl)benzodithiophene-2,6-diyl)-*alt*-[2,5-bis(3-dodecyl-thiophen-2-yl)thiazolothiazole-5,5'-diyl]}** (PBDTTT-TIPS). 2,6-Dibromo-4,8-bis(triisopropylsilyl)ethynylbenzo[1,2-*b*:4,5-*b'*]dithiophene (71 mg, 0.1 mmol) and 2,5-bis(3-dodecyl-5-(trimethylstannyl)thiophen-2-yl)thiazolo[5,4-*d*]thiazole (97 mg, 0.1 mmol) were dissolved in 10 mL of anhydrous toluene and deoxygenated with N<sub>2</sub> for 30 min. Pd(PPh<sub>3</sub>)<sub>4</sub> (11 mg, 0.01 mmol) was then added under N<sub>2</sub>. The mixture was stirred at reflux for 3 days. To end-cap the polymer chain, tributyl(thiophen-2-yl)stannane (3.7 mg, 0.01 mmol) was added under nitrogen, and the mixture was stirred at reflux for 10 h. 2-Bromothiophene (3.3 mg, 0.015 mmol) was then added under nitrogen, and the mixture was stirred at reflux for 10 h. After the reaction mixture was cooled to room temperature, the polymer was precipitated by addition of 80 mL of methanol. The precipitate was filtered. Finally, the polymer was purified by size exclusion gravity column chromatography over Bio-Rad Bio-Beads S-X1 (a kind of

Scheme 1. Synthetic Route of the Polymer

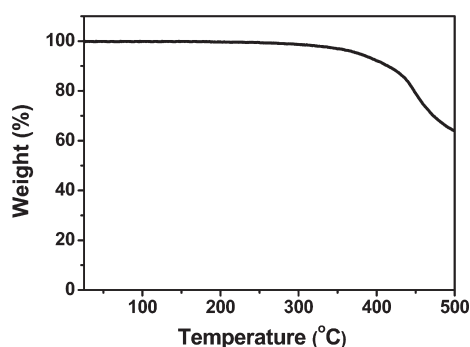
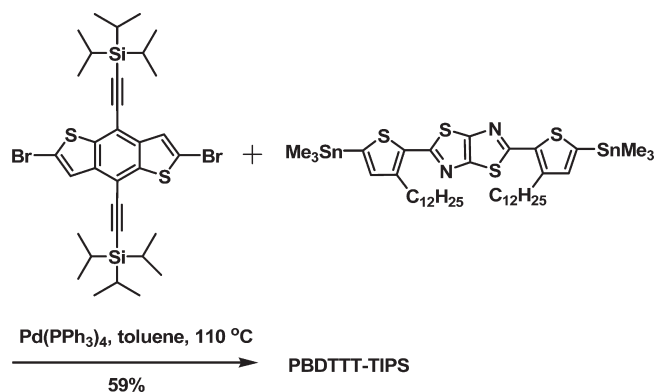


Figure 2. TGA curve of polymer PBDTTT-TIPS at a heating rate of 20 °C min<sup>-1</sup> under nitrogen.

porous cross-linked polystyrene polymers used for gel permeation separations of lipophilic polymers and low molecular weight, hydrophobic materials) eluting with chloroform. The polymer was recovered as a purple solid from the chloroform fraction by rotary evaporation (70 mg, 59%). <sup>1</sup>H NMR (400 MHz, CDCl<sub>3</sub>): δ 7.05 (br, 2H), 6.54 (br, 2H), 2.97 (br, 4H), 1.55–1.25 (br, 82H), 0.88 (br, 6H) (Figure S1, Supporting Information). GPC: *M<sub>n</sub>* 12 000; *M<sub>w</sub>* 19 000; *M<sub>w</sub>*/*M<sub>n</sub>* 1.6. Anal. Calcd for (C<sub>68</sub>H<sub>96</sub>N<sub>2</sub>S<sub>6</sub>Si<sub>2</sub>)<sub>*n*</sub>: C, 68.63; H, 8.13; N, 2.35. Found: C, 63.02; H, 7.72; N, 2.34%.

## RESULTS AND DISCUSSION

**Synthesis and Characterization.** Scheme 1 shows the synthetic route to PBDTTT-TIPS. Copolymerization of 2,6-dibromo-4,8-bis(triisopropylsilyl)benzo[1,2-*b*:4,5-*b'*]dithiophene and 2,5-bis(3-dodecyl-5-(trimethylstannyl)thiophen-2-yl)thiazolo[5,4-*d*]thiazole was carried out by Stille coupling reaction using Pd(PPh<sub>3</sub>)<sub>4</sub> as catalyst in toluene. The polymer was purified by size exclusion column chromatography over Bio-Rad Bio-Beads S-X1 eluting with chloroform. PBDTTT-TIPS is soluble in common organic solvents, such as chloroform, THF, chlorobenzene, and dichlorobenzene. Molecular weights of the polymer were determined by gel permeation chromatography (GPC) using polystyrene standards as calibrants. PBDTTT-TIPS has a number-average molecular weight (*M<sub>n</sub>*) of 12 000, weight-average molecular weight (*M<sub>w</sub>*) of 19 000, and polydispersity index (*M<sub>w</sub>*/*M<sub>n</sub>*) of 1.6. PBDTTT-TIPS shows excellent thermal stability with decomposition temperature of 377 °C (at 5% weight loss), as measured by thermogravimetric analysis

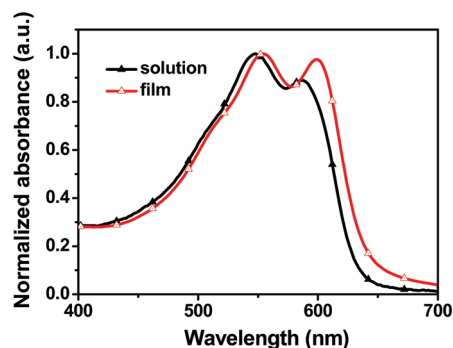


Figure 3. Absorption spectra of PBDTTT-TIPS in chloroform (10<sup>-6</sup> M) and in thin film (spin-coated from chloroform solution).

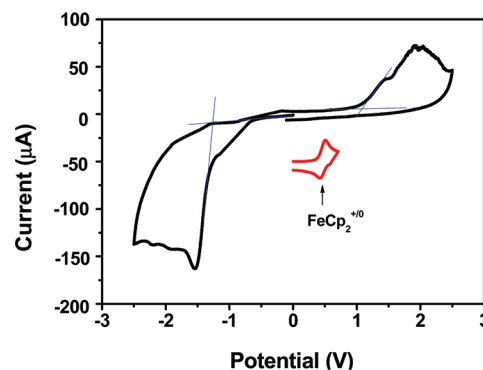
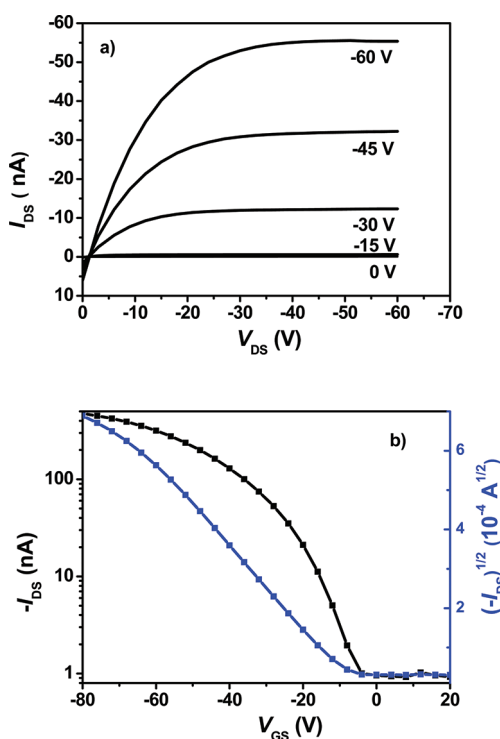


Figure 4. Cyclic voltammogram for PBDTTT-TIPS in CH<sub>3</sub>CN/0.1 M [tBu<sub>4</sub>N]<sup>+</sup>[PF<sub>6</sub>]<sup>-</sup> with ferrocenium/ferrocene as a standard, at 50 mV s<sup>-1</sup>. The horizontal scale refers to an anodized Ag wire pseudoreference electrode.

(TGA) at a heating rate of 20 °C min<sup>-1</sup> under nitrogen (Figure 2).

**Optical Properties.** Figure 3 shows the UV–vis absorption spectra of PBDTTT-TIPS in chloroform solution (10<sup>-6</sup> M) and in thin film (spin-coated from chloroform solution). The copolymer PBDTTT-TIPS in solution shows two intense absorption peaks at 548 and 586 nm, which red shift 6 and 12 nm from solution to film, respectively. Compared with PBDTTT-C12, PBDTTT-TIPS exhibits red-shifted absorption (4 nm in solution; 14 nm in film). The red shift of absorption for PBDTTT-TIPS mainly benefits from the weak electron-withdrawing and conjugated TIPS side chains. The optical bandgap of PBDTTT-TIPS estimated from the absorption edge in film is 1.94 eV, which is a little lower than that (1.99 eV) of PBDTTT-C12.

**Electrochemical Properties.** The cyclic voltammetry (CV) curves of copolymer PBDTTT-TIPS and FeCp<sub>2</sub><sup>+0</sup> are illustrated in Figure 4. PBDTTT-TIPS displays irreversible oxidation and reduction waves. The onset oxidation and reduction potentials versus Ag are 1.0 and -1.3 V, respectively. The onset oxidation and reduction potentials versus FeCp<sub>2</sub><sup>+0</sup> (half-wave potential of 0.5 eV) are 0.5 and -1.8 V, respectively. Therefore, the HOMO and LUMO energies are estimated to be -5.3 and -3.0 eV from the onset oxidation and reduction potentials, respectively, assuming the absolute energy level of FeCp<sub>2</sub><sup>+0</sup> to be 4.8 eV below vacuum. Compared with PBDTTT-TIPS, PBDTTT-C12 exhibits same HOMO level but 0.2 eV higher LUMO level. The trends in the electrochemical data are therefore consistent



**Figure 5.** (a) Typical current–voltage characteristics ( $I_{DS}$  vs  $V_{DS}$ ) at different gate voltages ( $V_{GS}$ ) and (b)  $-I_{DS}$  and  $(-I_{DS})^{1/2}$  vs  $V_{GS}$  plots at  $V_{DS}$  of  $-100$  V for a top contact device based on PBDTTT-TIPS in air.

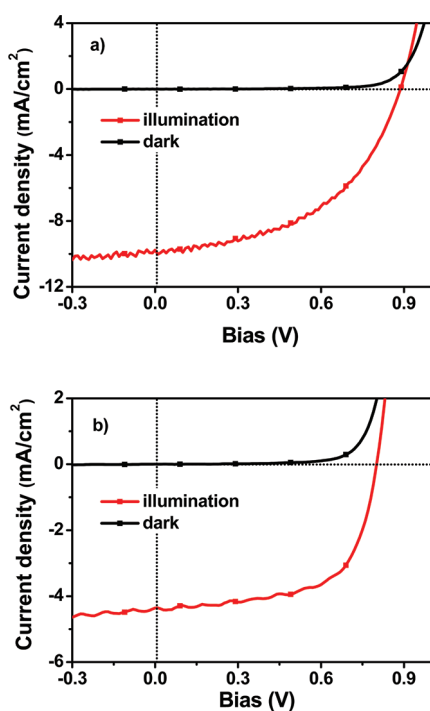


**Figure 6.** Current density–voltage characteristics of a device with the structure ITO/PEDOT:PSS/PBDTTT-TIPS:PC<sub>71</sub>BM(1:1, w/w)/Ca/Al (a) and ITO/PEDOT:PSS/PBDTTT-C12:PC<sub>71</sub>BM(1:2, w/w)/Ca/Al (b) under the illumination of an AM 1.5 solar simulator,  $100 \text{ mW cm}^{-2}$ .

with that in the absorption maxima and also can be attributed to the weak electron-withdrawing TIPS group. The lower

**Table 1.** Photovoltaic Performances of PSCs Based on PBDTTT-TIPS and PBDTTT-C12 under the Illumination of AM 1.5,  $100 \text{ mW cm}^{-2}$

active layer	$V_{oc}$ (V)	$J_{sc}$ ( $\text{mA cm}^{-2}$ )	FF (%)	PCE (%)
PBDTTT-TIPS:PC <sub>71</sub> BM = 1:1	0.89	9.77	49.8	4.33
PBDTTT-TIPS:PC <sub>71</sub> BM = 1:2	0.85	9.46	45.6	3.67
PBDTTT-C12:PC <sub>71</sub> BM = 1:2	0.80	4.36	62.8	2.19

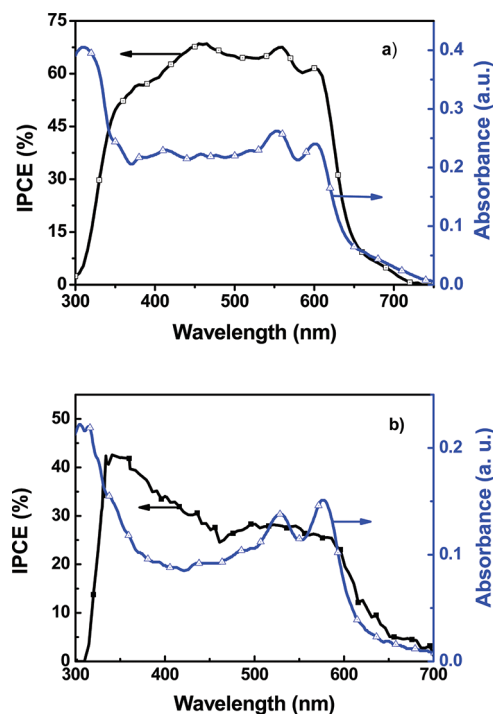


**Figure 7.** Absorption spectrum of a film of PBDTTT-TIPS:PC<sub>71</sub>BM-(1:1, w/w) (a) and PBDTTT-C12:PC<sub>71</sub>BM(1:2, w/w) (b) blend and IPCE curve as a function of wavelength.

LUMO level deduced from TIPS side chain was also reported in the literature.<sup>38</sup>

**Organic Field-Effect Transistors.** To ensure effective charge carrier transport to the electrodes and reduce the photocurrent loss in solar cells, the high hole mobility is a basic requirement for electron donors. To measure mobilities of PBDTTT-TIPS, organic field-effect transistors (OFETs) were fabricated on octadecyltrichlorosilane (OTS)-treated SiO<sub>2</sub>/Si substrates through spin-coating process. The typical p-type output curve and the corresponding transfer characteristics in air are depicted in Figure 5, which exhibits good current modulation and well-defined linear and saturation regions like PBDTTT-C12.<sup>42</sup> The highest hole mobility of the devices based on PBDTTT-TIPS in the saturation regime is  $1.2 \times 10^{-3} \text{ cm}^2 \text{ V}^{-1} \text{ s}^{-1}$ , while average mobility (5 devices) is  $9.4 \times 10^{-4} \text{ cm}^2 \text{ V}^{-1} \text{ s}^{-1}$ , a little lower but in the same order with that of PBDTTT-C12 ( $2.8 \times 10^{-3} \text{ cm}^2 \text{ V}^{-1} \text{ s}^{-1}$ ). The average on/off current ratio ( $I_{on}/I_{off}$ ) is 600.

**Photovoltaic Properties.** We use PBDTTT-TIPS as an electron donor and PC<sub>71</sub>BM as an electron acceptor and fabricate bulk heterojunction PSCs with a structure of ITO/PEDOT:PSS/PBDTTT-TIPS:PC<sub>71</sub>BM/Ca/Al to demonstrate the potential application of PBDTTT-TIPS in PSCs. The



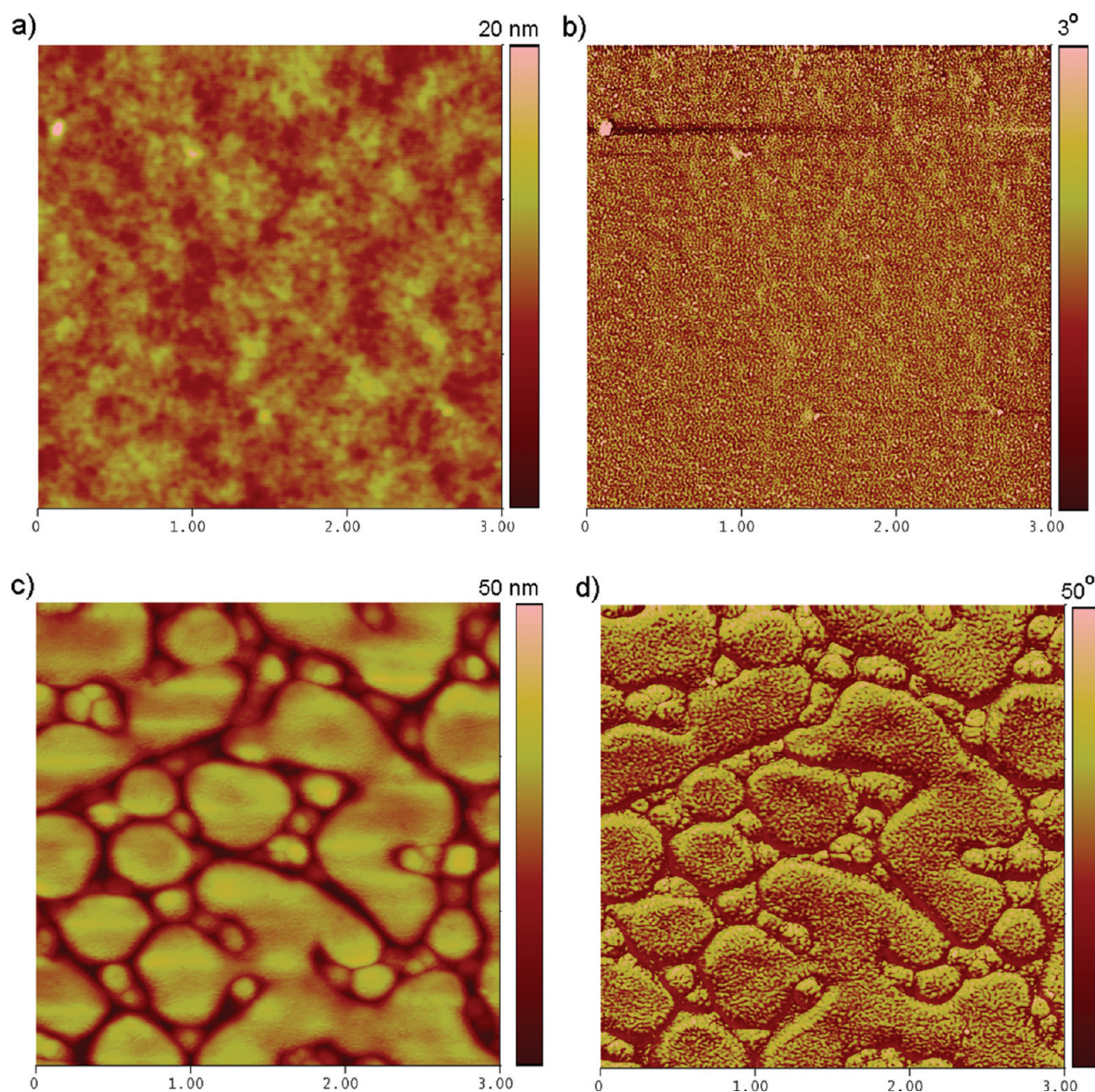


**Figure 8.** AFM topographic (left) and phase images (right) ( $3 \times 3 \mu\text{m}$ ) for thin films of PBDTTT-TIPS:PC<sub>71</sub>BM (1:1, w/w) (top) and PBDTTT-C12:PC<sub>71</sub>BM (1:2, w/w) blend (bottom).

solvents used for device fabrication will dramatically affect the morphology of blend film and the resulting device performance. Compared to PBDTTT-C12, PBDTTT-TIPS has a better solubility in common solvents, such as chloroform, THF, chlorobenzene, and dichlorobenzene. The PBDTTT-C12/PC<sub>71</sub>BM blend has good solubility in chloroform but poor solubility in chlorobenzene. Therefore, the best device performance based on PBDTTT-C12 was obtained from chloroform solution. However, the PBDTTT-TIPS/PC<sub>71</sub>BM blend has good solubility in chloroform and in chlorobenzene. The devices based on PBDTTT-TIPS:PC<sub>71</sub>BM = 1:1 spin-coated from chlorobenzene solution exhibited much higher PCE (4.33%) than that obtained from chloroform solution (1.3%) since the solvent with high boiling point would be more beneficial to forming good-quality films. Therefore, we choose chlorobenzene other than chloroform for PBDTTT-TIPS-based device fabrication.

Figure 6 shows current density–voltage curves, and Table 1 summarizes the open circuit voltage ( $V_{oc}$ ), short circuit current density ( $J_{sc}$ ), fill factor (FF), and power conversion efficiency (PCE) of the devices. When PBDTTT-TIPS:PC<sub>71</sub>BM weight ratio is 1:2, the PCE of device is 3.67%, which is higher than that for PBDTTT-C12-based device (2.19%). When PBDTTT-TIPS:PC<sub>71</sub>BM weight ratio is 1:1, the device exhibit the highest PCE of 4.33% with  $V_{oc}$  of 0.89 V,  $J_{sc}$  of  $9.77 \text{ mA cm}^{-2}$ , and FF of 49.8%. The change in performance with donor/acceptor weight ratio has correlation with the tendency of donor polymer to mix with fullerene acceptor, phase separation, and charge transport. Generally, for polymer donors with high hole mobilities ( $>10^{-3} \text{ cm}^2 \text{ V}^{-1} \text{ s}^{-1}$ ), such as poly(3-hexylthiophene) (P3HT) and PBDTTT-TIPS, the percolation pathways for hole transport are well formed at donor/acceptor weight ratio of 1:1, leading to higher PCEs. While for polymer donors with low hole mobilities

(<10<sup>-5</sup> cm<sup>2</sup> V<sup>-1</sup> s<sup>-1</sup>), such as poly[2-methoxy-5-(2'-ethyl-hexyloxy)-1,4-phenylenevinylene] (MEH-PPV), the percolation pathways for electron transport are well formed at high acceptor concentration (e.g., 80%), leading to higher PCEs.<sup>5</sup>

As shown in Figure 7, the incident photon to converted current efficiency (IPCE) curve resembles absorption spectrum of the blend thin film of PBDTTT-TIPS:PC<sub>71</sub>BM (1:1, w/w), and the IPCE exhibits a broad plateau with IPCE values over 50% between 350 and 620 nm, leading to a high  $J_{sc}$  of 9.77 mA cm<sup>-2</sup>. However, the PBDTTT-C12:PC<sub>71</sub>BM (1:2, w/w) blend gives a lower IPCE level between 300 and 700 nm, leading to a lower  $J_{sc}$  of 4.36 mA cm<sup>-2</sup>, which is only half of that for PBDTTT-TIPS:PC<sub>71</sub>BM device.

Although PBDTTT-TIPS and PBDTTT-C12 exhibit similar absorption, HOMO level, and hole mobility, they exhibit big difference in photovoltaic performance. To elucidate the origin, we investigate blend film morphology using atomic force microscope (AFM) (Figure 8). For PBDTTT-TIPS:PC<sub>71</sub>BM (1:1, w/w) blend, the films exhibit a typical cluster structure with many aggregated domains and a root-mean-square (rms) roughness of 1.472 nm. The domain sizes estimated by cross-section profiles are about 10–20 nm. Therefore, the nanoscale aggregated domains and perfect phase separation are beneficial to charge separation and enhanced efficiency of the PSC. In contrast, the PBDTTT-C12:PC<sub>71</sub>BM blend film exhibits large phase separation and large rms roughness up to 8.218 nm. This large phase separation scale is not favorable for efficient exciton dissociation, leading to relatively low  $J_{sc}$ . The blend film morphology indicates that PBDTTT-TIPS has a better compatibility with PC<sub>71</sub>BM than PBDTTT-C12. Nguyen et al. found that in a poly(3-alkylthiophenes)(P3AT):PC<sub>61</sub>BM system the longer side chains of P3AT enable the higher diffusion rate of PC<sub>61</sub>BM in the polymer matrix and ultimately lead to a larger scale phase separation.<sup>51</sup>

## CONCLUSIONS

A new conjugated copolymer PBDTTT-TIPS containing thiazolothiazole acceptor unit and TIPS-functionalized benzo-dithiophene donor unit is synthesized by Pd-catalyzed Stille coupling. PBDTTT-TIPS exhibits excellent thermal stability, broad absorption, high hole mobility, and relatively low HOMO level. Without any post-treatments, solution-processed PSCs based on the blend of PBDTTT-TIPS and PC<sub>71</sub>BM exhibit PCEs as high as 4.33%, which is 2 times that for device based on the PBDTTT-C12:PC<sub>71</sub>BM blend. TIPS and C12 side chains exhibit a little impact on absorption, HOMO level, and hole mobility of the polymers, but they exhibit significant impact on blend film morphology and photovoltaic performance. Relative to C12 side chains, TIPS side chains induced better compatibility between polymer donor and PC<sub>71</sub>BM; the PBDTTT-TIPS:PC<sub>71</sub>BM blend exhibits perfect phase separation with domain sizes around 10–20 nm, which is beneficial to charge separation and enhanced efficiency of the PSC.

## ASSOCIATED CONTENT

**S** Supporting Information. <sup>1</sup>H NMR spectrum of PBDTTT-TIPS. This material is available free of charge via the Internet at <http://pubs.acs.org>.

## AUTHOR INFORMATION

### Corresponding Author

\*E-mail: xwzhan@iccas.ac.cn.

### Notes

<sup>†</sup>Also at Graduate University of Chinese Academy of Sciences, Beijing 100049, China.

## ACKNOWLEDGMENT

This work was supported by NSFC (Grants 21025418, 51011130028, and 21021091), 973 Project (Grant 2011CB-808400), and the Chinese Academy of Sciences.

## REFERENCES

- (1) Arias, A. C.; MacKenzie, J. D.; McCulloch, I.; Rivnay, J.; Salleo, A. *Chem. Rev.* **2010**, *110*, 3.
- (2) Thompson, B. C.; Fréchet, J. M. J. *Angew. Chem., Int. Ed.* **2008**, *47*, 58.
- (3) Roncali, J. *Chem. Soc. Rev.* **2005**, *34*, 483.
- (4) Coakley, K. M.; McGehee, M. D. *Chem. Mater.* **2004**, *16*, 4533.
- (5) Gunes, S.; Neugebauer, H.; Sariciftci, N. S. *Chem. Rev.* **2007**, *107*, 1324.
- (6) Osaka, I.; McCullough, R. D. *Acc. Chem. Res.* **2008**, *41*, 1202.
- (7) Li, Y. F.; Zou, Y. P. *Adv. Mater.* **2008**, *20*, 2952.
- (8) Cheng, Y. J.; Yang, S. H.; Hsu, C. S. *Chem. Rev.* **2009**, *109*, 5868.
- (9) Zhao, X. G.; Zhan, X. W. *Chem. Soc. Rev.* **2011**, *40*, 3728.
- (10) Zhan, X. W.; Zhu, D. B. *Polym. Chem.* **2010**, *1*, 409.
- (11) Bundgaard, E.; Krebs, F. C. *Sol. Energ. Mater. Sol. Cells* **2007**, *91*, 954.
- (12) Chen, J. W.; Cao, Y. *Acc. Chem. Res.* **2009**, *42*, 1709.
- (13) Chen, H. Y.; Hou, J. H.; Zhang, S. Q.; Liang, Y. Y.; Yang, G. W.; Yang, Y.; Yu, L. P.; Wu, Y.; Li, G. *Nature Photonics* **2009**, *3*, 649.
- (14) Chu, T.-Y.; Lu, J.; Beaupré, S.; Zhang, Y.; Pouliot, J.-R. m.; Wakim, S.; Zhou, J.; Leclerc, M.; Li, Z.; Ding, J.; Tao, Y. *J. Am. Chem. Soc.* **2011**, *133*, 4250.
- (15) Price, S. C.; Stuart, A. C.; Yang, L.; Zhou, H.; You, W. *J. Am. Chem. Soc.* **2011**, *133*, 4625.
- (16) (a) Liang, Y.; Xu, Z.; Xia, J.; Tsai, S.-T.; Wu, Y.; Li, G.; Ray, C.; Yu, L. *Adv. Mater.* **2010**, *22*, E135. (b) Son, H. J.; Wang, W.; Xu, T.; Liang, Y.; Wu, Y.; Li, G.; Yu, L. *J. Am. Chem. Soc.* **2011**, *133*, 1885.
- (17) Zhou, H. X.; Yang, L. Q.; Stuart, A. C.; Price, S. C.; Liu, S. B.; You, W. *Angew. Chem., Int. Ed.* **2011**, *50*, 2995.
- (18) Huo, L. J.; Zhang, S. Q.; Guo, X.; Xu, F.; Li, Y. F.; Hou, J. H. *Angew. Chem., Int. Ed.* **2011**, *50*, 9697.
- (19) Price, S. C.; Stuart, A. C.; You, W. *Macromolecules* **2009**, *43*, 797.
- (20) Zhang, M.; Fan, H.; Guo, X.; He, Y.; Zhang, Z.-G.; Min, J.; Zhang, J.; Zhao, G.; Zhan, X.; Li, Y. *Macromolecules* **2010**, *43*, 8714.
- (21) Zhang, G.; Fu, Y.; Zhang, Q.; Xie, Z. *Chem. Commun.* **2010**, *46*, 4997.
- (22) Piliago, C.; Holcombe, T. W.; Douglas, J. D.; Woo, C. H.; Beaujuge, P. M.; Fréchet, J. M. J. *J. Am. Chem. Soc.* **2010**, *132*, 7595.
- (23) Fan, H. J.; Zhang, Z. G.; Li, Y. F.; Zhan, X. W. *J. Polym. Sci., Part A: Polym. Chem.* **2011**, *49*, 1462.
- (24) Li, Z.; Lu, J.; Tse, S.-C.; Zhou, J.; Du, X.; Tao, Y.; Ding, J. *J. Mater. Chem.* **2011**, *21*, 3226.
- (25) Wakim, S.; Alem, S.; Li, Z.; Zhang, Y.; Tse, S.-C.; Lu, J.; Ding, J.; Tao, Y. *J. Mater. Chem.* **2011**, *21*, 10920.
- (26) Liang, Y.; Feng, D.; Wu, Y.; Tsai, S.-T.; Li, G.; Ray, C.; Yu, L. *J. Am. Chem. Soc.* **2009**, *131*, 7792.
- (27) Shi, Q.; Fan, H.; Liu, Y.; Chen, J.; Ma, L.; Hu, W.; Shuai, Z.; Li, Y.; Zhan, X. *Macromolecules* **2011**, *44*, 4230.
- (28) Sista, P.; Nguyen, H.; Murphy, J. W.; Hao, J.; Dei, D. K.; Palaniappan, K.; Serrvello, J.; Kularatne, R. S.; Gnade, B. E.; Xue, B.



Dastoor, P. C.; Biewer, M. C.; Stefan, M. C. *Macromolecules* **2010**, *43*, 8063.

(29) Szarko, J. M.; Guo, J.; Liang, Y.; Lee, B.; Rolczynski, B. S.; Strzalka, J.; Xu, T.; Loser, S.; Marks, T. J.; Yu, L.; Chen, L. X. *Adv. Mater.* **2010**, *22*, 5468.

(30) Huo, L. J.; Hou, J. H.; Zhang, S. Q.; Chen, H. Y.; Yang, Y. *Angew. Chem., Int. Ed.* **2010**, *49*, 1500.

(31) Wang, M.; Hu, X.; Liu, P.; Li, W.; Gong, X.; Huang, F.; Cao, Y. *J. Am. Chem. Soc.* **2011**, *133*, 9638.

(32) Anthony, J. E. *Chem. Rev.* **2006**, *106*, 5028.

(33) Anthony, J. E. *Angew. Chem., Int. Ed.* **2008**, *47*, 452.

(34) Chung, D. S.; Park, J. W.; Yun, W. M.; Cha, H.; Kim, Y.-H.; Kwon, S.-K.; Park, C. E. *ChemSusChem* **2010**, *3*, 742.

(35) Winzenberg, K. N.; Kemppinen, P.; Fanchini, G.; Bown, M.; Collis, G. E.; Forsyth, C. M.; Hegedus, K.; Singh, T. B.; Watkins, S. E. *Chem. Mater.* **2009**, *21*, 5701.

(36) Park, J.-H.; Chung, D. S.; Lee, D. H.; Kong, H.; Jung, I. H.; Park, M.-J.; Cho, N. S.; Park, C. E.; Shim, H.-K. *Chem. Commun.* **2010**, *46*, 1863.

(37) Shu, Y.; Lim, Y.-F.; Li, Z.; Purushothaman, B.; Hallani, R.; Kim, J. E.; Parkin, S. R.; Malliaras, G. G.; Anthony, J. E. *Chem. Sci.* **2011**, *2*, 363.

(38) Wang, Y.; Parkin, S. R.; Watson, M. D. *Org. Lett.* **2008**, *10*, 4421.

(39) Ando, S.; Nishida, J. I.; Tada, H.; Inoue, Y.; Tokito, S.; Yamashita, Y. *J. Am. Chem. Soc.* **2005**, *127*, 5336.

(40) Osaka, I.; Zhang, R.; Sauve, G.; Smilgies, D. M.; Kowalewski, T.; McCullough, R. D. *J. Am. Chem. Soc.* **2009**, *131*, 2521.

(41) Osaka, I.; Sauve, G.; Zhang, R.; Kowalewski, T.; McCullough, R. D. *Adv. Mater.* **2007**, *19*, 4160.

(42) Shi, Q. Q.; Fan, H. J.; Liu, Y.; Hu, W. P.; Li, Y. F.; Zhan, X. W. *J. Phys. Chem. C* **2010**, *114*, 16843.

(43) Yang, M. A.; Peng, B.; Liu, B.; Zou, Y. P.; Zhou, K. C.; He, Y. H.; Pan, C. Y.; Li, Y. F. *J. Phys. Chem. C* **2010**, *114*, 17989.

(44) Huo, L.; Guo, X.; Zhang, S.; Li, Y.; Hou, J. *Macromolecules* **2011**, *44*, 4035.

(45) Zhang, M.; Guo, X.; Li, Y. *Adv. Energy Mater.* **2011**, *1*, 557.

(46) Zhang, Z. G.; Min, J.; Zhang, S. Y.; Zhang, J.; Zhang, M.; Li, Y. *Chem. Commun.* **2011**, *47*, 9474.

(47) Jung, I. H.; Yu, J.; Jeong, E.; Kim, J.; Kwon, S.; Kong, H.; Lee, K.; Woo, H. Y.; Shim, H. K. *Chem.—Eur. J.* **2010**, *16*, 3743.

(48) Lee, S. K.; Cho, J. M.; Goo, Y.; Shin, W. S.; Lee, J.-C.; Lee, W.-H.; Kang, I.-N.; Shim, H.-K.; Moon, S.-J. *Chem. Commun.* **2011**, *47*, 1791.

(49) Subramaniyan, S.; Xin, H.; Kim, F. S.; Shoaee, S.; Durrant, J. R.; Jenekhe, S. A. *Adv. Energy Mater.* **2011**, *1*, 854.

(50) Heeney, M.; Zhang, W.; Tierney, S.; McCulloch, I. WO 2008/011957.

(51) Nguyen, L. H.; Hoppe, H.; Erb, T.; Gunes, S.; Gobsch, G.; Sariciftci, N. S. *Adv. Funct. Mater.* **2007**, *17*, 1071.